Journal of Power Sources 199 (2012) 350–354

Contents lists available at SciVerse ScienceDirect

Journal of Power Sources

journal homepage: www.elsevier.com/locate/jpowsour

Short communication

Facile synthesis of VO_2(B)/carbon nanobelts with high capacity and good cyclability

Qianqian Zhao, Lifang Jiao*, Wenxiu Peng, Haiyan Gao, Jiaqin Yang, Qinghong Wang, Hongmei Du, Li Li, Zhan Qi, Yuchang Si, Yijing Wang, Huatang Yuan

Institute of New Energy Material Chemistry, Key Laboratory of Advanced Energy Materials Chemistry (MOE), Tianjin Key Lab of Metal and Molecule-based Material Chemistry, MOE (IRT-0927), Nankai University, Tianjin 300071, PR China

ARTICLE INFO

Article history:
Received 25 July 2011
Received in revised form 14 October 2011
Accepted 17 October 2011
Available online 20 October 2011

Keywords:
Hydrothermal synthesis
Metastable vanadium dioxide/carbon nanobelts
Cathode material
Lithium ion batteries

ABSTRACT

Metastable vanadium dioxide/carbon (VO_2(B)/C) nanobelts have been successfully synthesized via a facile surfactant-free hydrothermal method using V_2O_5 and sucrose as reactants. The VO_2(B)/C with carbon content of 0.96 wt.% shows well-distributed nanobelt morphology with an average width of 120–200 nm, thickness of 40–60 nm and length of 1–3 μm. The nanobelts exhibit preferable electrochemical performances with high initial discharge capacity, good cycling stability and excellent high-rate performance. The initial discharge capacity can reach 218.6 mAh g^{-1}, and maintain 152.6 mAh g^{-1} after 100 cycles at 50 mA g^{-1}. When the current density increases to 1000 mA g^{-1}, the discharge capacity is still as high as 138.2 mAh g^{-1}. VO_2(B)/C nanobelts would be a promising cathode material for lithium ion batteries.

1. Introduction

Among all the cathode materials of lithium ion batteries, vanadium oxides have attracted great attention. As we all know, vanadium exists with a wide range of oxidation states from +2 to +5. Meanwhile, the vanadium oxides have a lot of merits and have been widely used in catalysts [1], chemical sensors [2], lithium ion batteries [3] and magnesium batteries [4–6]. As an important functional metal oxide, vanadium dioxide with a layered structure possesses excellent physical and chemical properties [7,8]. VO_2 exhibits four different polymorphic structures, including the most stable VO_2(R) with rutile structure, the monoclinic VO_2(R) with a slightly distorted rutile structure, a tetragonal structure of VO_2(A) and the metastable VO_2(B) with a monoclinic structure [9]. Especially, VO_2(B) with metastable monoclinic structure is a promising cathode material for both organic and aqueous lithium ion batteries [3,8–15] owing to its proper electrode potential and tunnel structure [16].

Nanostructured materials have exhibited special physical and chemical properties due to their nanometer-size dimensions [17]. It was reported that nanostructured vanadium oxides can enhance the electrochemical properties compared with their bulk counterparts [11,18]. In recent years, great efforts have been made to synthesis VO_2(B) nanomaterials with different morphologies, such as nanorods [19,20], nanoribbons [21,22], nanotubes [23,24], and nanowires [25]. The nanostructured morphology greatly improves the initial discharge capacity of VO_2(B) materials [19]. However, the poor cycling performance of VO_2(B) nanomaterial greatly limits its practical applications [19,20]. The capacity fading is probably due to the large specific surface areas and high surface energies, which makes it easier to aggregate together during charge/discharge process, thus increases the charge transfer resistance [26].

Literatures have proposed that carbon dispersed in the electrode materials can provide a pathway for electron transport, resulting in improvement of the electronic conductivity [27,28]. Herein, we introduce a simple hydrothermal approach for the synthesis of VO_2(B)/carbon nanobelts with good electrochemical performances using V_2O_5 and sucrose as reactants. Sucrose is a cheap and environmentally friendly reagent. During the synthesis, sucrose acts as reductant and carbon source, without adding foreign surfactants or hazard reducing reagents. The synthetic approach has the merits of simplicity, low-cost, convenience and environmentally benign. Moreover, the obtained products have high discharge capacity, excellent cycling stability, and high-rate performances, which make it a potential candidate as electrode materials in lithium ion batteries.

2. Experimental

2.1. Preparation and structural characterization

All the reagents were used without further purification. The VO_2(B)/C composites were prepared by a facile one-pot

* Corresponding author. Tel.: +86 22 23498089; fax: +86 22 23502604.
E-mail address: jiaolf@nankai.edu.cn (L. Jiao).

0378-7753/$ – see front matter © 2011 Elsevier B.V. All rights reserved.
doi:10.1016/j.jpowsour.2011.10.067

hydrothermal synthesis. In a typical procedure, different amounts of sucrose (0.0238, 0.0475, 0.0713, 0.0950 g) were dissolved in 70 mL deionized water, then 0.1 g V_2O_5 was added into the above solution and stirred for 2 h until the V_2O_5 powder dispersed uniformly. The yellow mixture was subsequently transformed into a Teflon lined autoclave with a stainless steel shell. The autoclave was maintained at 180 °C for 12 h and then cooled to room temperature naturally. The resulting blue-black precipitates were washed with distilled water and absolute ethanol thoroughly. Finally, the samples were dried in vacuum at 60 °C for 10 h for further characterizations. The products obtained were named as S1, S2, S3 and S4.

The crystal structure of the as-prepared samples was characterized by X-ray diffraction (XRD, Rigaku.D/Max III) using Cu Kα radiation (λ = 1.5418 Å) in a 2θ range from 10° to 80° at room temperature. The morphology and microstructure were observed by scanning electron microscopy (SEM, JEM-6700F) and transmission electron microscopy (TEM, Tecnai 20). The carbon content was analyzed by a Perkin-Elmer 2400 Series II CHNS/O elemental analyzer.

2.2. Electrochemical measurements

The electrochemical properties of VO_2(B)/C composites were evaluated in Li test cell. The electrodes were fabricated by mixing active materials, acetylene black and polyvinylidene fluoride (PVDF) binder in a weight ratio of 80:15:5 in N-methyl-pyrrolidinone (NMP) solvent to form homogeneous slurry, and then the mixtures were coated on an Al foil which had been cut into circular flakes of 8 mm in diameter. The circular strips were dried at 60 °C for 12 h in vacuum oven. The testing cells were assembled with the electrodes thus fabricated, metallic lithium anode, Celgard 2320 film separator and 1 M $LiPF_6$ in 1:1:1 ethylene carbonate (EC)/dimethyl carbonate (DMC)/ethylene methyl carbonate (EMC) electrolyte. The cells were assembled in an argon filled glove box, where water and oxygen concentration was kept less than 5 ppm. The cells were discharged and charged on Land CT2001 automatic battery tester between 1.5 and 4.0 V vs. Li/Li^+. Cyclic voltammograms (CV) was tested with a scan rate of 0.1 mV s^{-1} between 1.5 and 4.0 V.

3. Results and discussion

3.1. Characterization of structure and morphology

Fig. 1 presents the typical XRD patterns of the samples obtained at 180 °C for 12 h with different amounts of sucrose. When the sucrose is few (for S1), the impurity phase of $V_3O_7{\cdot}H_2O$ is detected. With the increase of sucrose content (from S2 to S4), the impurity phase disappears and the intensity of the diffraction peaks of VO_2(B) strengthens. It can be clearly seen that the diffraction peaks of S3 are the strongest, indicating the best crystallinity. However, too much sucrose (0.0950 g) decreases the crystallinity of the sample, just as the XRD pattern of S4. As depicted in Fig. 1, the diffraction peaks from S2 to S4 can be indexed to the monoclinic structure of VO_2(B) (space group *C*2/*m*, JCPDS No. 81-2392). No typical diffraction peaks of carbon are found, so carbon yielded from the carbonization of sucrose should exist in amorphous form. Elemental analysis displays that the carbon content of S2 to S4 are 0.81, 0.96 and 1.46 wt.%, respectively.

The SEM images of as-synthesized VO_2(B)/C samples are demonstrated in Fig. 2. S1 is composed of nanorods and big blocks which aggregate together, while S2 is composed of nanobelts and micrograins. S3 is composed of nanobelts with good dispersion. For S4, it

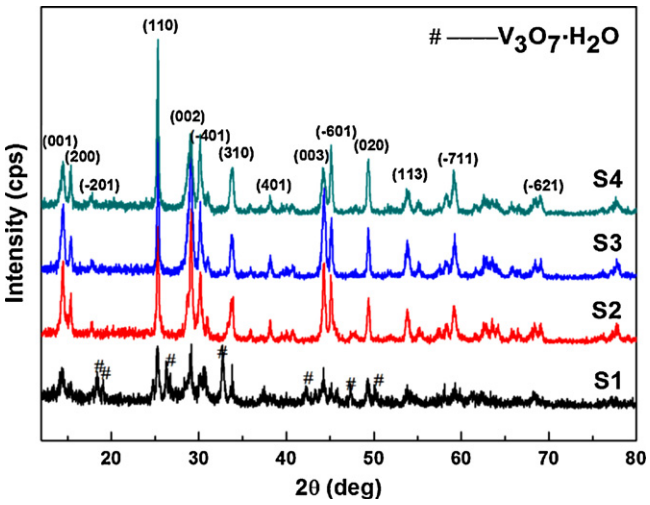

Fig. 1. X-ray diffraction patterns of VO_2(B)/C composites (S1–S4).

is assembled by nanobelts and uneven grains which group together. It is obvious that the size of sample S3 is the smallest. Also, in all the products, the distribution of S3 is uniform, which implies that it may have good electrochemical properties.

Fig. 3 displays the representative SEM, TEM and HRTEM images of S3. As shown in Fig. 3a, the composite exhibits a belt-like morphology. These nanobelts are about 1–3 μm long with smooth surface, typically 120–200 nm wide and 40–60 nm thick. Fig. 3b gives the TEM image of nanobelts structure of S3 which is consistent with Fig. 3a. To gain insight into the structure of the prepared nanobelts, HRTEM is performed on an individual nanobelt. Typical HRTEM image (Fig. 3c) of S3 exhibits lattice fringes clearly, where the lattice planes with a *d* spacing of 0.352 nm corresponding to the (1 1 0) planes, which is consistent with monoclinic VO_2(B) (JCPDS No. 81-2392), as confirmed by XRD.

3.2. Electrochemical properties

Fig. 4a shows the cycle performances of the VO_2(B)/C composites at a discharge current density of 50 mA g^{-1}. From S2 to S4, the initial discharge capacities are 216, 218.6 and 217.3 mAh g^{-1}, respectively, while the discharge capacities maintain 116.2, 152.6 and 132.8 mAh g^{-1} after 100 cycles. The initial discharge capacity of S3 is much higher than VO_2(B) nanorods (152 mAh g^{-1}) [20] and VO_2(B)/C core–shell microspheres of (187 mAh g^{-1}) [29]. The capacity retentions of S2 to S4 are 53.8%, 69.8% and 61.1%, respectively, and obviously S3 is the highest. The 100th discharge capacity of S3 is 36.4 mAh g^{-1} higher than S2 and 19.8 mAh g^{-1} than S4. The above statistics indicate that S3 has the best cycling stability (corresponding to the formation of $Li_{0.68}VO_2$). Fig. 4b compares the charge/discharge curves of S3 in the 1st, 2nd, 3rd, 50th and 100th cycle. All charge/discharge curves are similar with flat plateaus, corresponding to lithium extraction and intercalation reactions. The initial discharge capacity of S3 is 218.6 mAh g^{-1} and it still remains 218.5, 205.2, 163.6 and 152.6 mAh g^{-1} at the 2nd, 3rd, 50th and 100th cycle, respectively. The discharge capacity retention rate is 69.8% after 100 cycles, which is much higher than S2 (53.8%) and S4 (61.1%) samples.

The rate properties of S2–S4 tested between 1.5 and 4.0 V are displayed in Fig. 5. Obviously, S3 has the best rate capability. The first discharge capacity of S3 at 50 mA g^{-1} is 220.2 mAh g^{-1}, and maintains 213.8 mAh g^{-1} at the 10th cycle, with the capacity retention of 97.1%. The capacity retention is high and this trend continues up to 60 cycles. Even at the current density of 1000 mA g^{-1}, the discharge capacity can still reach 138.2 mAh g^{-1}. The capacity

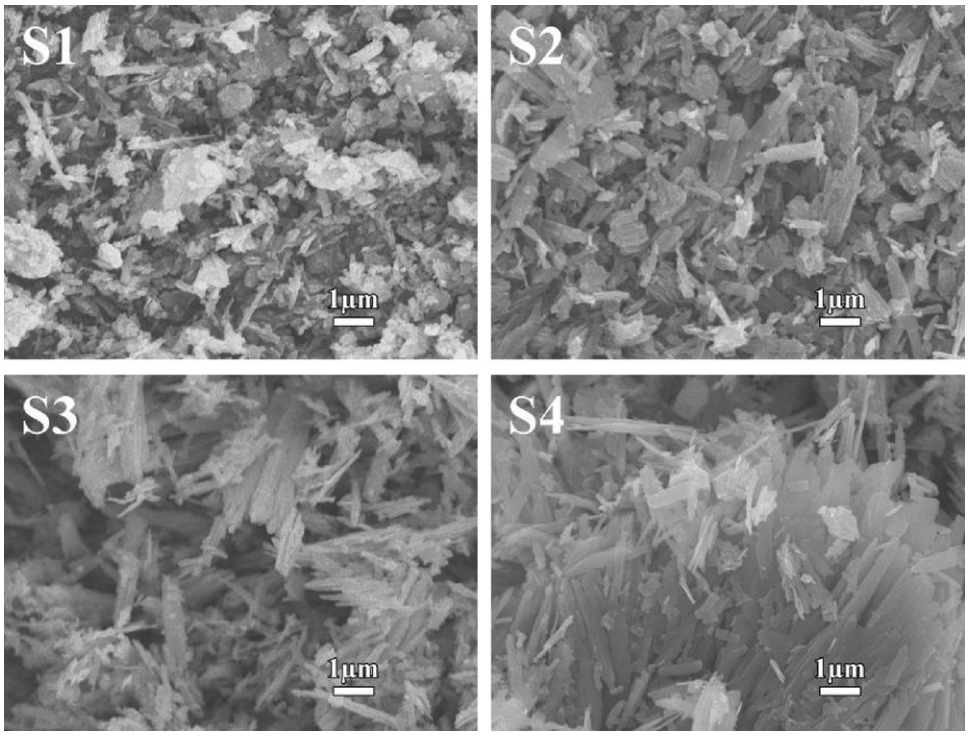

Fig. 2. SEM images of VO_2(B)/C composites (S1–S4).

retention of S3 measured at every 10 cycles is 85.1% at 100 mA g^{-1}, 80% at 200 mA g^{-1}, 69.3% at 500 mA g^{-1}, 58.1% at 1000 mA g^{-1} and 75.7% at 50 mA g^{-1} of the initial discharge capacity. While returning to 50 mA g^{-1}, the S3 electrode maintains a discharge capacity of 175.7 mA g^{-1} (79.8% of initial discharge capacity), manifesting good reversibility.

The unfavorable factor affecting VO_2(B) as cathode materials is its unsatisfying cyclability. Nano-size materials have been prepared by researchers to improve the cycle performance of VO_2(B). Chen et al. [19] and Subba Reddy et al. [20] have synthesized VO_2(B) nanorods, and the reported initial discharge capacities are 605 and 152 mAh g^{-1} while the capacity retentions are 24.8% (30 cycles) and 49.3% (17 cycles), respectively. The nanorods undergo serious capacity loss during the cycling process. The bad cyclability of the nanorods may be caused by the aggregation of active materials during the cycling process. To further improve the

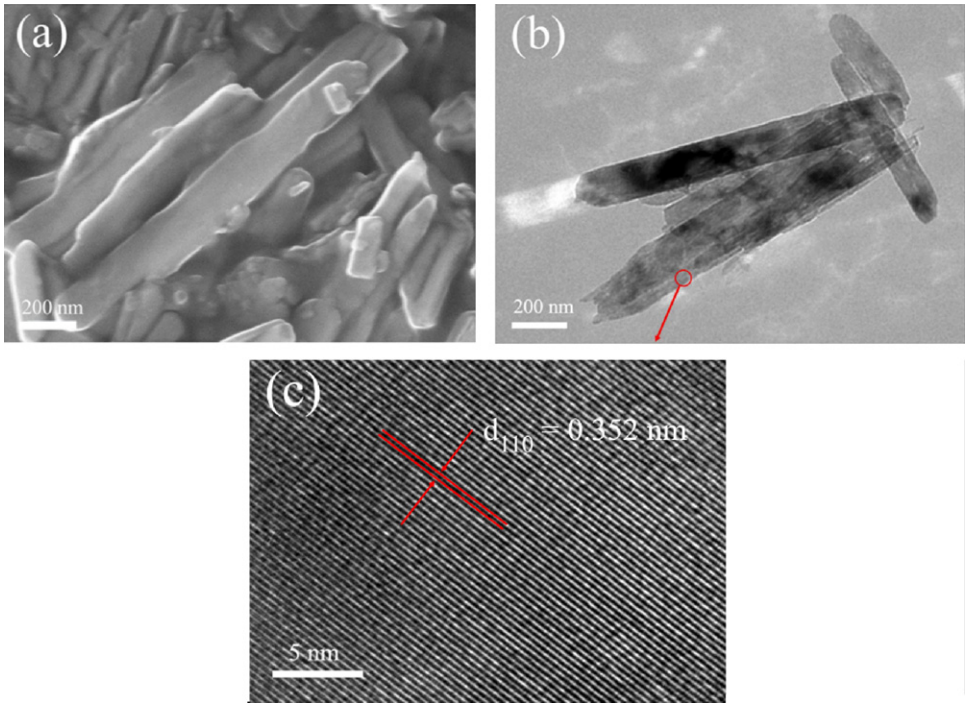

Fig. 3. Typical SEM, TEM and HRTEM images of S3 nanobelts. (a) SEM, (b) TEM and (c) HRTEM.

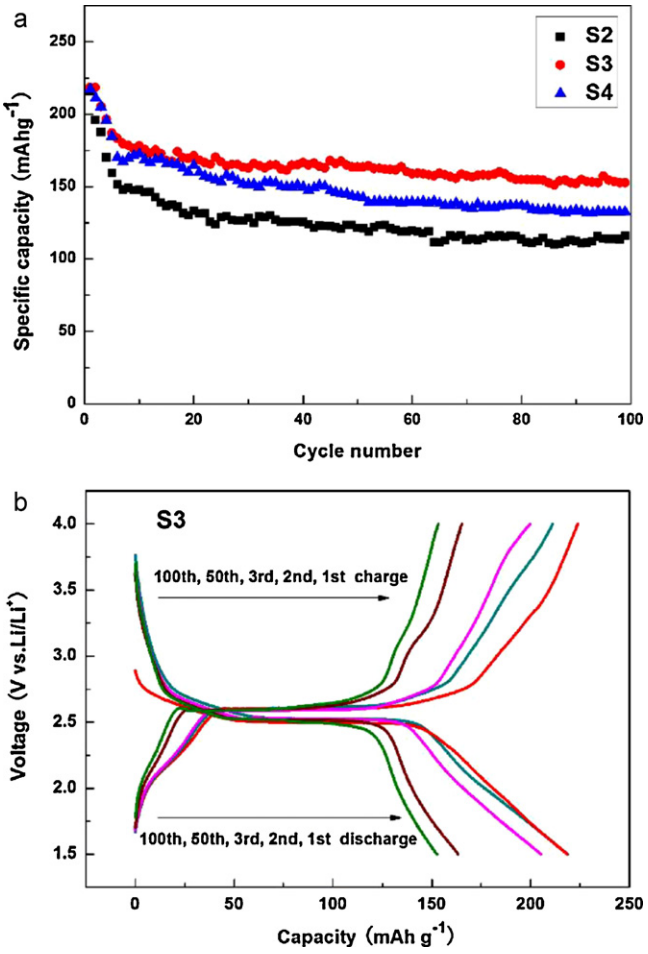

Fig. 4. (a) Cyclic performances of VO_2(B)/C composites (S2–S4) at a current density of 50 mA g^{-1} between 1.5 and 4.0 V, (b) charge/discharge curves of S3.

cyclability, VO_2(B)/C core–shell microspheres were fabricated with the initial discharge capacity of 180 mAh g^{-1} [29] and the capacity retention raised to 51% after 50 cycles. The unsatisfying capacity retention may be due to its micro-size structure and large content of carbon (42 wt.%). In this paper, the capacity retention of S3 is 69.8% after 100 cycles, which is much higher than the nanorods [19,20] and the core–shell microspheres [29]. The good cyclic performance of VO_2(B)/C nanobelts may be due to its uniform nanobelt

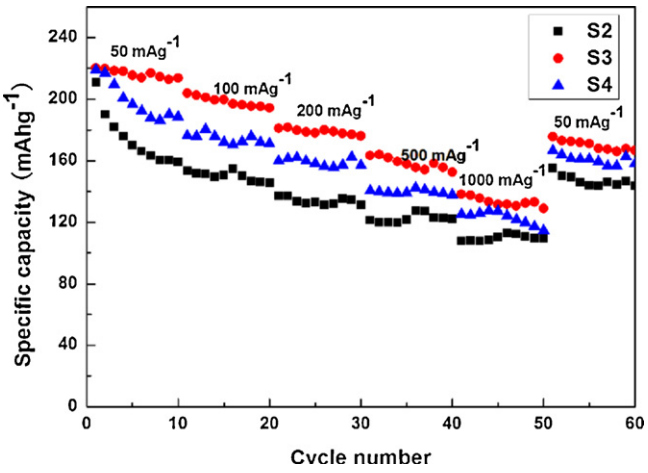

Fig. 5. Cyclic performances of VO_2(B)/C composites (S2–S4) electrodes at different current densities.

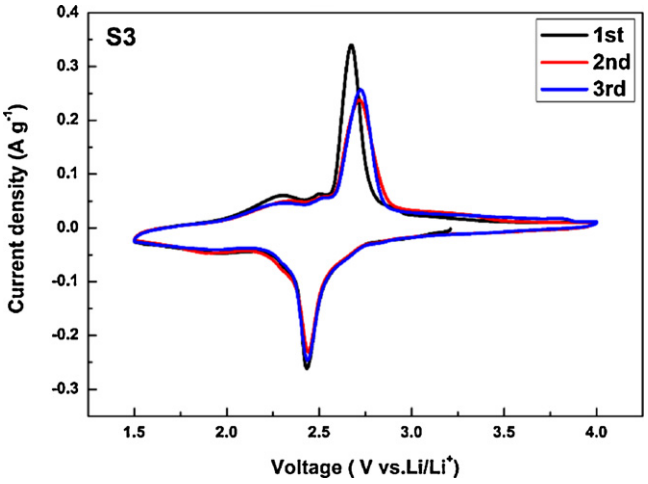

Fig. 6. Cyclic voltammograms (CV) of S3 at the first three cycles.

structure and proper content of carbon (0.96 wt.%), which prevent the aggregation of active material and accommodate the large volume variation and maintain good electronic contact [8].

The CV curves of S3 during the first three cycles are shown in Fig. 6, in the potential range of 1.5–4.0 V at a scan rate of 0.1 mV s^{-1}. It can be obviously obtained that there is mainly a pair of redox peaks for each cycle. For the first cycle, during the cathodic scan, an intensity peak is observed at 2.43 V, indicating the insertion of Li^+. During the first anodic scan (Li^+ extraction), the CV shows two low-intensity peaks at 2.28 V and 2.5 V followed by an intensity peak at 2.67 V. The two weak peaks may be due to the oxidation process of low-valent vanadium oxides with low content which is reduced by carbon. The main redox peak potentials are consistent with the literature [8] and the charge/discharge plateaus. The second and third cathodic scans are analogous to the first cathodic scan with the peak potential located at 2.43 V. The second and third anodic scans of S3 slightly differ from the first anodic one. The anodic peak at 2.67 V is shifted to a higher potential (2.72 V) with the increase of the cycle number. The positive shift of oxidation peak potential may be attributed to the structure change and polarization of the electrode after the first charge/discharge process. CV curves of the second and the third cycles overlap, indicating that the S3 product has good stability and reversibility for the insertion and extraction of lithium ions.

4. Conclusions

In this study, VO_2(B)/C composites were successfully synthesized using a one-pot surfactant-free hydrothermal method with V_2O_5 and different amounts of sucrose as reactants. The results turned out that when the carbon content was 0.96 wt.% (the mass of sucrose was 0.0713 g), the VO_2(B)/C nanobelts show the most stable cyclability (152.6 mAh g^{-1} at 50 mA g^{-1} after 100 cycles) and high-rate discharge capacity (138.2 mAh g^{-1} at 1000 mA g^{-1}). Thus, this work provides a facile route to synthesize VO_2(B)/C nanobelts with excellent electrochemical performances as potential cathode material in lithium ion batteries.

Acknowledgments

This work was financially supported by 973 program (2010CB631303), NSFC (20801059, 21073100), TSTC (10JCYBJC08000, 11JCYBJC07200), Tianjin Sci & Tech (10SYSYJC27600) and MOE Innovation Team (IRT0927).

References

[1] N. Magg, B. Immaraporn, J.B. Giorgi, T. Schroeder, M. Baumer, J. Dobler, Z. Wu, E. Kondratenko, M. Cherian, M. Baerns, P.C. Stair, J. Sauer, H.J. Freund, J. Catal. 226 (2004) 88–100.
[2] P. Liu, S.H. Lee, H.M. Cheong, C.E. Tracy, J.R. Pitts, R.D. Smith, J. Electrochem. Soc. 49 (2002) H76–H80.
[3] C. Tsang, A. Manthiram, J. Electrochem. Soc. 144 (1997) 520.
[4] L.F. Jiao, H.T. Yuan, Y.C. Si, Y.J. Wang, Y.M. Wang, Electrochem. Commun. 8 (2006) 1041–1044.
[5] L.F. Jiao, H.T. Yuan, Y.J. Wang, J.S. Cao, Y.M. Wang, Electrochem. Commun. 7 (2005) 431–436.
[6] H.X. Li, L.F. Jiao, H.T. Yuan, M. Zhang, J. Guo, L.Q. Wang, M. Zhao, Y.M. Wang, Electrochem. Commun. 8 (2006) 1693–1698.
[7] Y.P. Ma, W. Xue, Z.-C. Wang, M.F. Ge, S.G. He, J. Phys. Chem. A112 (2008) 3731–3741.
[8] M.M. Rahmana, J.Z. Wang, N.H. Idris, Z.X. Chen, H.K. Liu, Electrochim. Acta 56 (2010) 693–699.
[9] T. Chirayil, P.Y. Zavalij, M.S. Whittingham, Chem. Mater. 10 (1998) 2629–2640.
[10] R. Li, C.Y. Liu, Mater. Res. Bull. 45 (2010) 688–692.
[11] N. Ding, X.Y. Feng, S.H. Liu, J. Xu, X. Fang, I. Lieberwirth, C.H. Chen, Electrochem. Commun. 11 (2009) 538–541.
[12] G. Armstrong, J. Canales, A.R. Armstrong, P.G. Bruce, J. Power Sources 178 (2008) 723–728.
[13] S.D. Zhang, Y.M. Li, C.Z. Wu, F. Zheng, Y. Xie, J. Phys. Chem. C 113 (2009) 15058–15067.
[14] W.T. Jiang, J. Ni, K. Yu, Z.Q. Zhu, Appl. Surf. Sci. 257 (2011) 3253–3258.
[15] J. Ni, W.T. Jiang, K. Yu, Y.F. Gao, Z.Q. Zhu, Electrochim. Acta 56 (2011) 2122–2126.
[16] D.W. Murphy, P.A. Christian, F.J. Disalvo, J.N. Carides, J.V. Waszczak, J. Electrochem. Soc. 128 (1981) 2053–2060.
[17] A.P. Alivisators, Science 271 (1996) 933.
[18] K.H. Seng, J. Liu, Z.P. Guo, Z.X. Chen, D.Z. Jia, H.K. Liu, Electrochem. Commun. 13 (2011) 383–386.
[19] Z.J. Chen, S.K. Gao, L.L. Jiang, M.D. Wei, K.M. Wei, Mater. Chem. Phys. 121 (2010) 254–258.
[20] Ch.V. Subba Reddy, E.H. Walker Jr., S.A. Wicker Sr., Q.L. Williams, R.R. Kalluru, Curr. Appl. Phys. 9 (2009) 1195–1198.
[21] L.J. Mao, C.Y. Liu, Mater. Res. Bull. 43 (2008) 1384–1392.
[22] G.C. Li, S.P. Pang, L. Jiang, Z.Y. Guo, Z.K. Zhang, J. Phys. Chem. B 110 (2006) 9383–9386.
[23] M. Niederberger, H.-J. Muhr, F. Krumeich, F. Bieri, D. Gunther, R. Nesper, Chem. Mater. 12 (2000) 1995–2000.
[24] F. Krumeich, H.-J. Muhr, M. Niederberger, F. Bieri, B. Schnyder, R. Nesper, J. Am. Chem. Soc. 121 (1999) 8324–8331.
[25] X.Y. Chen, X. Wang, Z.H. Wang, J.X. Wan, J.W. Liu, Y.T. Qian, Nanotechnology 15 (2004) 1685–1687.
[26] H.M. Liu, Y.G. Wang, K.X. Wang, E. Hosono, H.S. Zhou, J. Mater. Chem. 19 (2009) 2835–2840.
[27] H. Huang, S.C. Yin, L.F. Nazar, Electrochem. Solid State Lett. 4 (2001) A170.
[28] Z. Chen, J.R. Dahn, J. Electrochem. Soc. 149 (2002) A1184.
[29] F. Wang, Y. Liu, C.Y. Liu, Electrochim. Acta 55 (2010) 2662–2666.